Conformational changes induced by phosphorylation of the FixJ receiver domain

Catherine Birck, Lionel Mourey, Patrice Gouet, Béatrice Fabry, Jörg Schumacher, Philippe Rousseau, Daniel Kahn, Jean-Pierre Samama

Conformational changes induced by phosphorylation of the FixJ receiver domain

Catherine Birck[1†], Lionel Mourey[1†], Patrice Gouet[1], Béatrice Fabry[1], Jörg Schumacher[2], Philippe Rousseau[2], Daniel Kahn[2] and Jean-Pierre Samama[1*]

Background: A variety of bacterial adaptative cellular responses to environmental stimuli are mediated by two-component signal transduction pathways. In these phosphorelay cascades, histidine kinases transphosphorylate a conserved aspartate in the receiver domain, a conserved module in the response regulator superfamily. The main effect of this phosphorylation is to alter the conformation of the response regulator in order to modulate its biological function. The response regulator FixJ displays a typical modular arrangement, with a phosphorylatable N-terminal receiver domain and a C-terminal DNA-binding domain. In the symbiotic bacterium *Sinorhizobium meliloti*, phosphorylation of this response regulator activates transcription of nitrogen-fixation genes.

Results: The crystal structures of the phosphorylated and of the unphosphorylated N-terminal receiver domain of FixJ (FixJN) were solved at 2.3 Å and 2.4 Å resolution, respectively. They reveal the environment of the phosphoaspartate in the active site and the specific conformational changes leading to activation of the response regulator. Phosphorylation of the conserved aspartate induces major structural changes in the β4–α4 loop, and in the signaling surface α4–β5 that mediates dimerization of the phosphorylated full-length response regulator. A site-directed mutant at this protein–protein interface decreases the affinity of the phosphorylated response regulator for the *fixK* promoter tenfold.

Conclusions: The cascade of phosphorylation-induced conformational changes in FixJN illustrates the role of conserved residues in stabilizing the phosphoryl group in the active site, triggering the structural transition and achieving the post-phosphorylation signaling events. We propose that these phosphorylation-induced conformational changes underly the activation of response regulators in general.

Addresses: [1]Groupe de Cristallographie Biologique, CNRS-IPBS, 205 route de Narbonne, 31077-Toulouse, France and [2]Laboratoire de Biologie Moléculaire des Relations Plantes-Microorganismes, UMR 215 INRA-CNRS, Chemin de Borde Rouge, BP27, Castanet-Tolosan CEDEX, France.

*Corresponding author.
E-mail: samama@ipbs.fr

[†]These authors contributed equally to this work.

Key words: nitrogen-fixation regulation, phosphorylation, response regulator, signaling surface, X-ray structure

Received: 9 August 1999
Revisions requested: 13 September 1999
Revisions received: 23 September 1999
Accepted: 4 October 1999

Published: 26 November 1999

Structure December 1999, 7:1505–1515

0969-2126/99/$ – see front matter

Introduction

Signal transduction in two-component systems is mediated by Mg^{2+}-dependent phosphorelay reactions between protein histidine kinases and phosphoaccepting receiver domains in response regulator proteins [1]. Most response regulators are modular proteins, and the phosphorylation state of the receiver domain controls the activity of the additional domains that display DNA-binding or enzymatic properties. Genetic, biochemical and structural approaches have suggested that the main effect of phosphorylation is to alter the conformation of the response regulators and to modulate the signaling activity by selective protein–protein interactions. For some response regulators phosphorylation may also promote the formation of oligomeric species required for their biological functions [2]. The three-dimensional structures of unphosphorylated response regulators [3–10] illustrated the conserved doubly wound five-stranded α/β fold of receiver domains and the similarity of the active sites containing a conserved lysine and three carboxylic acids (including the phosphorylatable aspartate residue). This argued for a common mechanism of phosphorylation for all members of the response regulator superfamily [3,11,12]. The half-lives of phosphorylated proteins range from a few seconds to many minutes [13–15]. The hydrolysis of the acylphosphate groups is catalysed by the autophosphatase activity of the response regulators, which ensures that the proteins are not permanently activated. This property, which may be stimulated by protein partners in the signaling circuit, is evidently crucial to their *in vivo* signaling roles.

FixL/FixJ is the oxygen-sensitive two-component system involved in the regulation of symbiotic nitrogen fixation in *Sinorhizobium meliloti* [16,17]. Under microaerobic conditions, the kinase FixL phosphorylates the response regulator FixJ so that it activates transcription of the *nifA* and *fixK* genes. Fix J binding sites have been found at upstream positions in the promoters of these genes.

Sequence conservation was revealed in the –54 to –33 region of four FixJ-dependent promoters [18]. A high-affinity region located between –69 and –44 overlaps with a lower-affinity region between position –57 and –31 in the *fixK* promoter. Both binding sites are protected by phosphorylated FixJ [19]. Under aerobic conditions the unphosphorylated protein is essentially inactive [17,19–21]. FixJ displays a typical modular arrangement, with a phosphorylatable N-terminal receiver domain and a C-terminal transcriptional-activator domain [22,23]. The FixJ receiver domain inhibits the latent activity of the C-terminal domain within the native protein, and this inhibition is relieved by phosphorylation of the receiver domain. Phosphorylation also induces dimerization of the response regulator, a process mediated by the receiver domain that significantly enhances the affinity of the response regulator for the *fixK* promoter [24]. Phosphorylation was postulated to cause a conformational change in the receiver domain that has not been understood until now.

In this paper we present the X-ray structures of the receiver domain of FixJ in its unphosphorylated and phosphorylated forms. We observed major displacements in the β4–α4–β5 region, particularly in the β4–α4 loop, resulting in the reorientation of helix α4. These phosphorylation-induced conformational changes have a profound impact on the signaling surface of the receiver domain and allow formation of the functional dimers.

Table 1

Data collection and refinement statistics for unphosphorylated FixJN.

Datasets	Native	Samarium	Platinum
Data collection			
Resolution limit (Å)	30.0–2.4	30.0–2.4	30.0–1.9
Measured reflections	15,435	26,081	30,758
Unique reflections	8231	8265	15,980
Completeness* (%) overall/last shell	98.0/95.3	98.0/95.6	94.0/93.5
R_{sym}* (%) overall/last shell	2.1/6.3	5.0/13.2	4.0/15.7
R_{iso} (%)	-	27.0	29.0
R_{cullis} (iso/ano)	-	0.8/0.6	0.9/-
Phasing power (iso/ano)	-	1.5/1.8	1.1/-
Refinement			
Resolution (Å)	15.0–2.4	15.0–2.4	
No. of molecules in the AU	2	2	
No. of protein atoms	1793	1852	
No. of samarium ions	-	4	
No. of solvent molecules	49	75	
No. of other heteroatoms†	19	19	
No. of reflections work/test	7455/858	7383/862	
Crystallographic R factor/R_{free}	0.21/0.27	0.196/0.265	
Mean temperature factor (Å^2)	17	22	

*The resolution ranges in highest bin are 2.49–2.4 Å and 1.97–1.9 Å for native and samarium, and for platinum, respectively. †An ordered segment of 19 atoms of PEG has been positioned. AU is asymmetric unit.

Results and discussion

Structure determination

The unphosphorylated N-terminal receiver domain of FixJ (FixJN, residues 1–126) crystallized in the triclinic space group with two molecules in the asymmetric unit. The crystal structure of the protein was solved and refined at 2.4 Å resolution using multiple isomorphous replacement with anomalous scattering (MIRAS) phasing with platinum and samarium heavy-atom derivatives (Table 1). Phosphorylation of FixJN by acetylphosphate led to dimeric species, which were separated from the unphosphorylated protein by chromatographic methods. The half-life of the phosphorylated FixJN dimer (approximately two hours) in the presence of Mg^{2+} could be increased to several months by removal of the metal ion with EDTA [25] and storage in appropriate conditions (see the Materials and methods section). This allowed the screening of crystallization conditions in which the addition of the detergent Triton X-100 was critical to obtain single crystals with good diffraction quality. Addition of Triton X-100 to phosphorylated dimers did not affect the properties of the phosphorylated species according to gel-filtration and small-angle X-ray scattering (SAXS) analysis. The dephosphorylation process induced by addition of Mg^{2+} to these species was similar to that occurring from phosphorylated dimers purified in the absence of EDTA. The phosphorylated FixJN dimer crystallized in the monoclinic C2 space group. The structure of the phosphorylated species was solved by molecular replacement using the structure of the unphosphorylated FixJN monomer as a model, and was refined at 2.3 Å resolution. The R and R_{free} values were 0.217 and 0.244, respectively (Table 2). There are three molecules of phosphorylated FixJN per asymmetric unit, named the ABC assembly. The crystallographic twofold axis duplicates this motif and leads to the

Table 2

Data collection and refinement statistics for phosphorylated FixJN.

Data collection	
Resolution limit (Å)	24.5–2.3
Measured reflections	83,599
Unique reflections overall	26,027
Completeness* (%) overall/last shell	89.8/92.8
R_{sym}* (%) overall/last shell	5.0/15.5
Refinement	
Resolution (Å)	24.5–2.3
No. of molecules in the AU	3
No. of protein atoms	2802
No. of atoms in phosphoryl groups	12
No. of solvent molecules water/sulfate	144/4
No. of reflections work/test	24,811/1188
Crystallographic R factor/R_{free}	0.217/0.244
Mean temperature factor (Å^2)	42.3

*The resolution range in highest bin is 2.42–2.3 Å.

tandem repeat CBAABC, the building unit of the crystal lattice, formed by three functional dimers (CB, AA and BC). The two protomers in the AA dimer are related by the crystallographic twofold axis and are therefore strictly identical. The protomers B and C in the BC dimers are related by a noncrystallographic twofold axis. Pairwise superposition of protomers A, B and C gives root mean square deviation (rmsd) values for the C_α atoms of 0.20 Å, 0.40 Å and 0.40 Å for A versus B, A versus C and B versus C, respectively. Superposition of the AA and BC dimers gives rmsd values for the C_α atoms of 0.56 Å. Taking into account the estimated coordinate errors at this resolution (0.30 Å), these rmsd values indicate that the differences between dimers in the unit cell are not significant. The electron density is well defined in both structures and does not suggest higher mobility of specific regions in the unphosphorylated or in the phosphorylated protein.

Overview of the phosphorylated FixJN dimer

Each phosphorylated receiver domain of FixJ adopts the doubly wound five-stranded α/β fold classically found in the other response regulators of known structures (Figure 1). The dimerization of the phosphorylated receiver domain produces a new molecular species of dimensions 52 × 26 × 28 Å (Figure 2). In this assembly the two receiver modules have the same orientation and all helices and strands, except α1 and β2, run in the same direction, nearly perpendicular to the rather flat surface of the dimer where the two active sites are located.

The active sites in FixJN and phospho-FixJN

The structures of the unphosphorylated metal-free FixJN and Sm^{3+}-bound protein were similar and will be described in detail elsewhere. The Sm^{3+}-bound protein illustrates the prephosphorylation state of the protein. The Sm^{3+} ion is

Figure 1

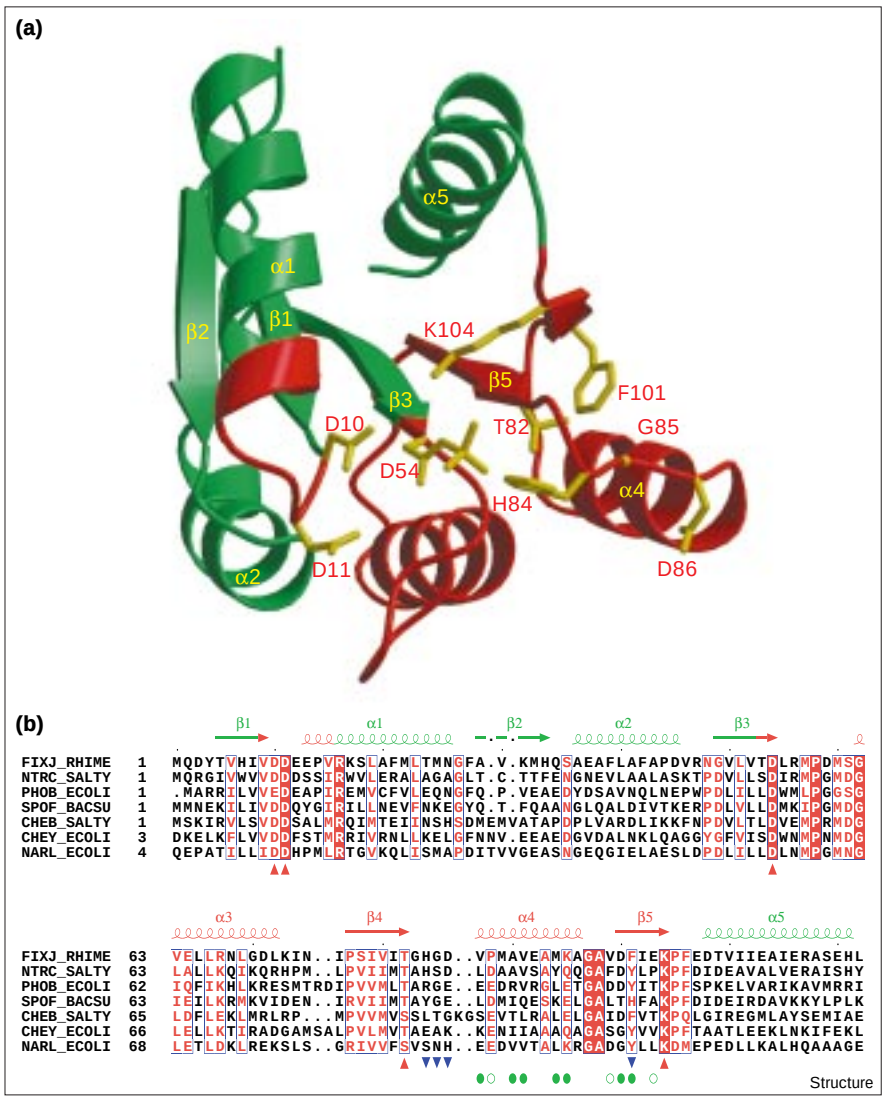

Phosphorylated FixJN structure. (a) Ribbon diagram of phosphorylated FixJN. The secondary structure elements are labeled. The regions that are most similar in the phosphorylated and unphosphorylated states are shown in green and those that are significantly affected by phosphorylation are shown in red. The residues in the active-site region and those that move by more than 4 Å upon phosphorylation are represented. (b) Structure-based sequence alignment of FixJN against other receiver domains of known structure: *S. meliloti* FixJN (this work), *Salmonella typhimurium* NtrC [5], *E. coli* PhoB [10], *Bacillus subtilis* Spo0F [6,8], *S. typhimurium* CheB [9], *E. coli* CheY [3,56] and *E. coli* NarL [7]. The secondary structure elements of FixJN are indicated by coils for α helices and arrows for β sheets, with the same color code as in (a). Homologous residues are in red and identical residues are shown as white letters on a red background. Conserved residues in the active-site region are marked with red triangles. Residues that move by more than 4 Å upon phosphorylation are indicated by blue triangles. Residues of phosphorylated FixJN involved in the dimer interface are indicated by solid green circles (high contribution) and open green circles (low contribution). The receiver domains are listed in decreasing order of identity and similarity scores with FixJN from NtrC (34.5% identity, 57.7% similarity) to NarL (23.2% identity, 51.7% similarity). Figures 1b and 7 were created using ESPript [57].

Figure 2

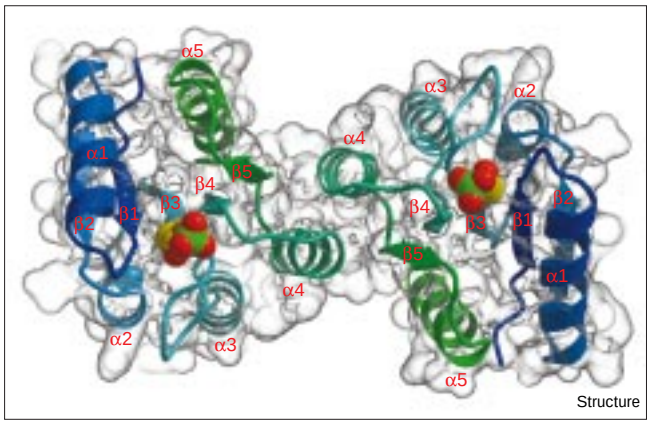

View of the phosphorylated FixJN dimer. Each protomer is represented by ribbons and the color varies from dark blue (N terminus) to green (C terminus). The secondary structure elements are labeled and the phosphoaspartate groups are shown as spheres. The van der Waals surface of the dimer generated using SURFNET [58] is shown as a transparent solid.

bound in the active site and liganded to the mainchain oxygen atom of Arg56 and to the carboxylic oxygen atoms of Asp11 and Asp54 (Figure 3a). This geometry is identical to that displayed by the Mg^{2+} and Mn^{2+} ions bound in the active sites of the unphosphorylated receiver domains [3,4,26]. The Lys104 sidechain points into the active site, at 4.5 Å from the carboxylic group of Asp54.

In the dimer of phospho-FixJN, each molecule of the receiver domain is phosphorylated on Asp54 (Figure 3b). The phosphorous atom is covalently linked to an oxygen atom of the carboxylate group and the three phosphoryl oxygen atoms O1, O2 and O3 form numerous polar interactions (Figure 3c). The O1 atom is found at 2.9 Å and 3.1 Å from the mainchain nitrogen atom of Gly83 and from the ammonium group of Lys104, respectively. The O2 atom is at hydrogen-bonding distance from the mainchain nitrogen atom of Arg56 (2.8 Å) and the Og1 atom of Thr82 (2.8 Å). It is also in van der Waals contact with the imidazole ring of His84. The O3 atom interacts with a water molecule and with a species located in the acidic pocket. This species could possibly be an ammonium ion provided by the crystallization medium, as the geometry and distances to its protein-atom ligands (Asp10, Asp11, Glu12, Asp54 and the mainchain oxygen atom of residue 56) are extremely similar to those found for an ammonium ion bound to parvalbumin in a crystal structure solved at 0.9 Å resolution (Protein Data Bank [PDB] code 2PVB).

Except for the van der Waals contact with the His84 sidechain, all the interactions made by the phosphoryl group in the active site involve mainchain atoms of the protein and the sidechain atoms of two residues highly conserved in the response regulator superfamily (Thr82 and Lys104). It suggests that the environment of the acylphosphate group in phospho-FixJ is conserved in other receiver domains. Indeed, these essential sidechains are known to contribute to the functional properties of various response regulators [27–31]. The conformational change of FixJN upon phosphorylation provides some insight into these contributions.

The phosphorylation-induced conformational changes

The unphosphorylated and phosphorylated receiver domains were compared after superposition of C_α atoms of the 62 residues that were, according to δ-distance plot calculations, minimally affected by phosphorylation of the protein (Figure 4a). The rmsd over these 62 C_α atoms was 0.3 Å. On the basis of this superposition, the rmsd was 1.1 Å over all atoms of these 62 residues and 1.7 Å over all protein atoms. This suggests that the conformational change upon phosphorylation propagates throughout the whole domain in line with the results from nuclear magnetic resonance (NMR) spectroscopic investigations of phosphorylated CheY [32,33] and of mutant proteins of the receiver domain of NtrC, which mimic the effect of phosphorylation [34].

The phosphorylation event induces major structural changes in two regions. The first one involves all residues from position 53 in strand β3 to position 105 at the C-terminal end of strand β5 (Figure 4b). The second region is from residue 9 at the C-terminal edge of strand β1 to residue 15 in the first turn of helix α1. These effects are correlated and seem to be primarily driven by the movement of Thr82. The formation of a strong hydrogen bond between the acylphosphate group and the Thr82 sidechain induces a significant modification of the mainchain dihedral angle of this residue, which, in turn, affects the loop that connects β4 and α4 (residues 83–86). The conformational change of this loop is drastic, and the shift in position for the mainchain atoms of residues 84 and 85 amounts to 6 Å (Figure 4b). Gly83, His84, Gly85 and Asp86, which form a type II β turn in the unphosphorylated protein, adopt a nearly fully extended conformation in the phosphorylated receiver domain, which pushes the N-terminal part of helix α4 away from the active site by 4.5 Å (Figure 4c). The movement of the Thr82 sidechain by 2.3 Å towards the active site, in the opposite direction to the displacement of helix α4, creates a cavity between β4 and α4 that is filled by the aromatic ring of Phe101 in the phosphorylated form (Figure 4c). From the unphosphorylated to the phosphorylated states the sidechain of Phe101 rotates from its outwards orientation to an internal rotamer towards the protein core. The phenyl ring forms van der Waals contacts with the sidechain of Leu55 at the C-terminal edge of β3. In order to avoid steric clashes, the movement of Phe101 towards Leu55 requires the displacement of the mainchain of residues 53–58, and, in

Figure 3

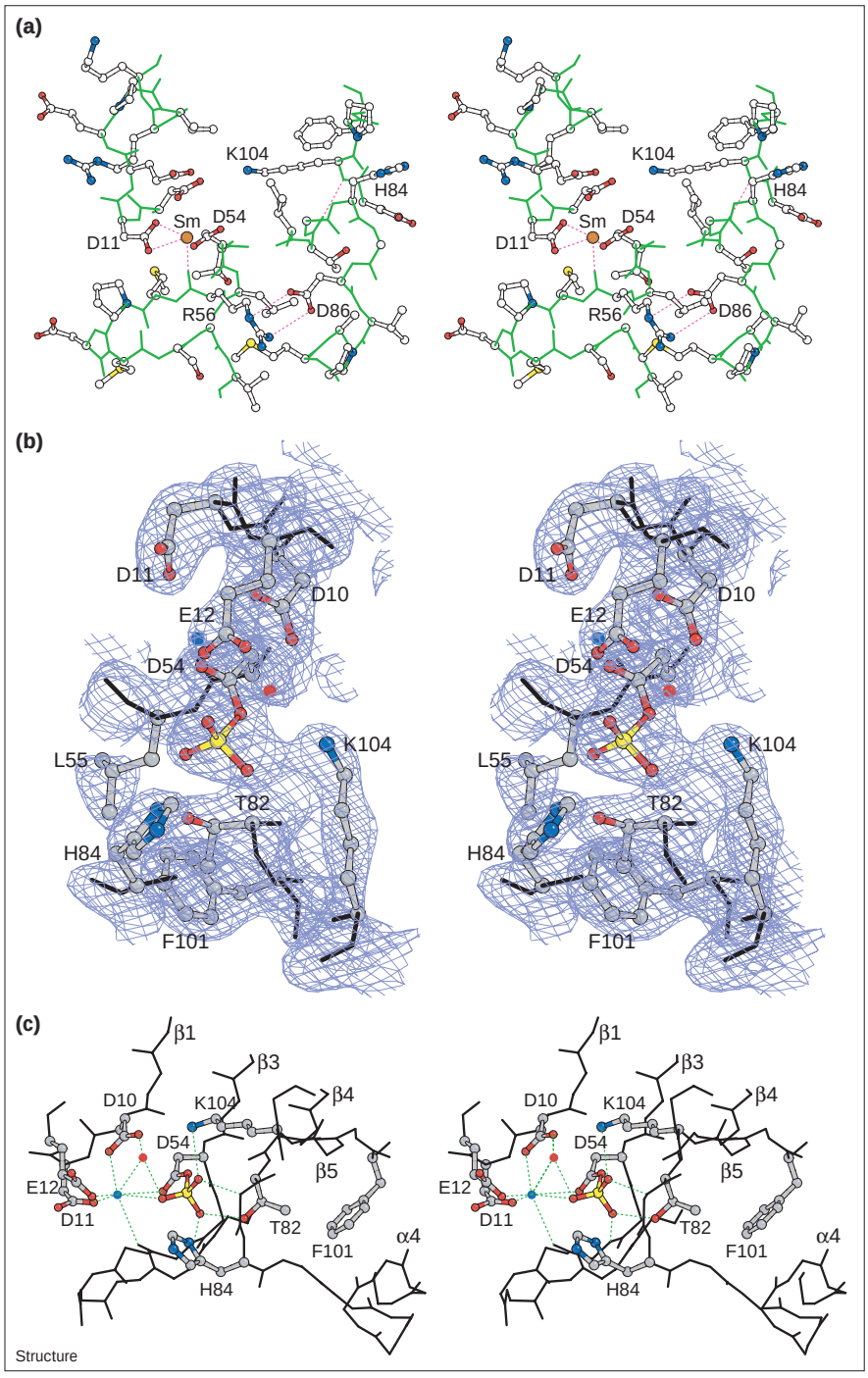

Active sites of unphosphorylated and phosphorylated FixJN. (a) Stereoview of the active-site environment of unphosphorylated FixJN showing the Sm^{3+} ion (orange) bound in the acidic pocket. The conformation of the connecting loop β4–α4 is stabilized by the interactions between Arg56 and Asp86. Selected polar interactions are shown as pink dotted lines. Oxygen, nitrogen and sulfur atoms are in red, blue and yellow, respectively. (b) Stereoview of the final electron-density map of phosphorylated FixJN (SIGMAA weighted $2F_o–F_c$ map contoured at 1.5σ) illustrating the acylphosphate group of Asp54 and the neighboring sidechains. (c) Stereoview of the active site of phosphorylated FixJN showing the environment of the phosphoryl group and the orientation of Phe101. The hydrogen-bonding interactions made by the acylphosphate group, the water molecule (red dot) and the ammonium ion (blue dot) in the active site are represented by green dotted lines.

turn, that of residue 9 in the adjacent β1 strand (Figure 4c). The reorientation of Phe101 alters the main-chain conformation of the β5 strand in its central part.

The main features of the cascade of conformational changes we observed in FixJN are likely to occur upon phosphorylation of other response regulators. Indeed, biochemical and genetic studies on mutant proteins have emphasized the essential role of the conserved serine or threonine residue (Thr82 in FixJ), and it has been concluded that the hydroxyl group of this residue may be necessary for a post-phosphorylation signaling event. This is the case in FixJ. The direct interaction between the hydroxyl group of Thr82 and the phosphoryl group

Figure 4

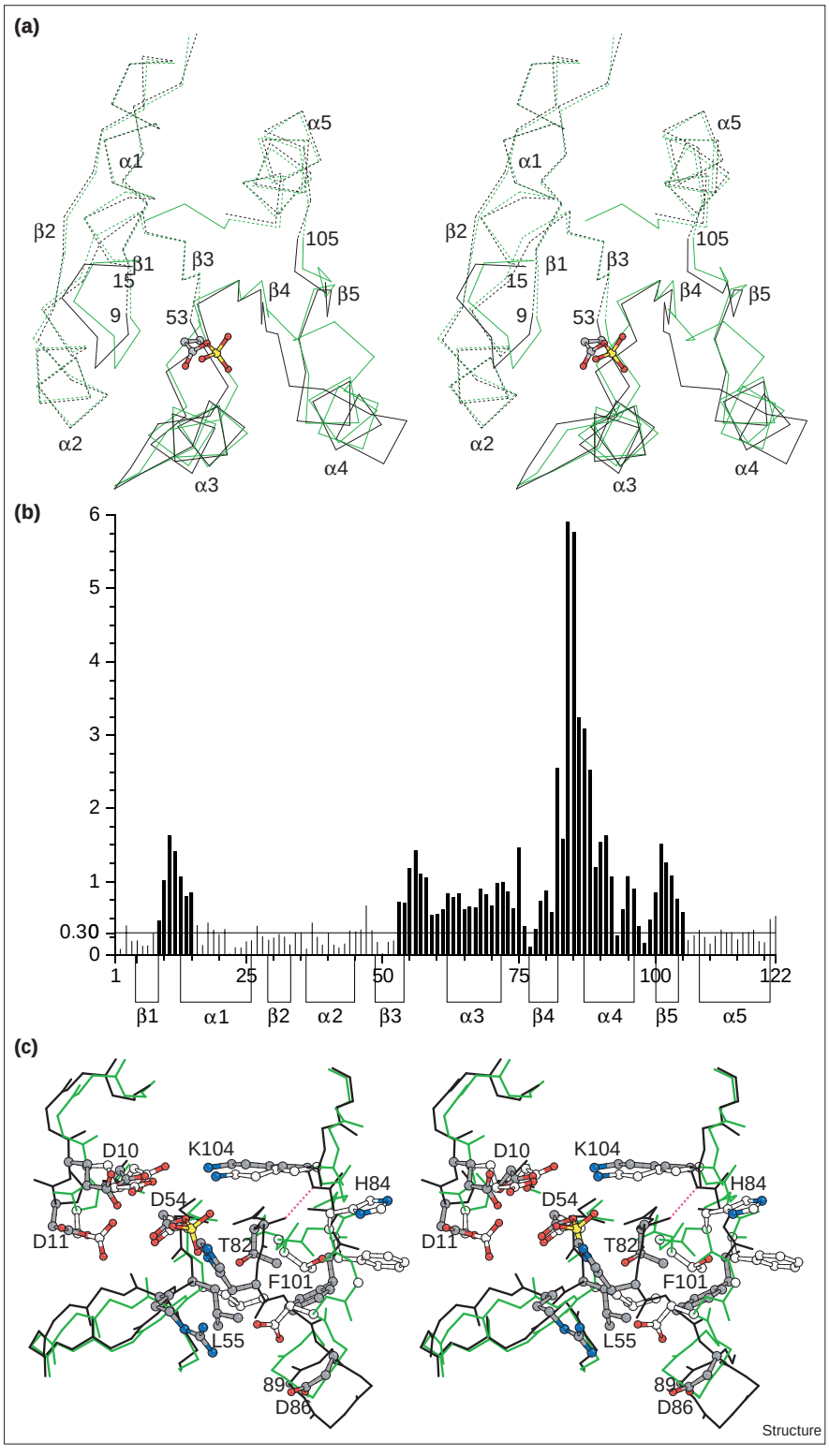

Phosphorylation-induced conformational changes. **(a)** Stereoview of the mainchain traces of the unphosphorylated (green) and phosphorylated (black) FixJN structures. The 62 C_α atoms represented by dotted lines are least influenced by phosphorylation of the protein (rmsd = 0.3 Å) according to δ-distance plot calculations. These atoms were used for superposition of the two structures. The C_α atoms that undergo conformational changes upon phosphorylation are represented by continuous lines. The acylphosphate group is in ball and stick representation. **(b)** Magnitude of the C_α shifts for all residues of the receiver domain. The thin and thick lines correspond to the dotted and continuous representations in (a), respectively. The secondary structure elements are indicated. **(c)** Stereoview of the active-site environments in the unphosphorylated (green backbone atoms and open bonds for sidechains) and phosphorylated (black backbone atoms and grey bonds for sidechains) states. The hydrogen bond between the mainchain oxygen atom of Thr82 and the mainchain nitrogen atom of Lys104 is indicated by a pink dotted line. The superposition of the two structures was performed as indicated in (a).

may, in addition, contribute to stabilizing the phosphorylated species. This would explain the low amount of phosphorylated T82I (single-letter amino acid code) mutant protein [29] as, according to the structure of unphosphorylated FixJN and to those of other receiver domains, this mutation should not interfere with the

chemistry of phosphotransfer to Asp54. A similar situation may occur in Spo0F where the threonine to alanine mutation also impairs phosphorylation of the receiver domain by phospho-KinA [30]. A different case is offered by the T87I and T87A mutants of CheY, which are readily phosphorylated by the kinase CheA. Lys109 (Lys104 in FixJ, the second sidechain interacting with the acylphosphate group) may provide sufficient interactions to the phosphoryl group in these proteins [27] in which the nonchemotactic properties may result from an impaired cascade of conformational changes.

The dimer interface of phospho-FixJN

The phosphorylation-induced conformational changes of region 53–105 lead to the molecular definition of the dimer interface provided by helix α4 and strand β5 from each receiver domain (Figure 2). Their relatedness by a twofold axis implies identical interactions between protomers. The protein–protein interface involves van der Waals interactions provided by the sidechains of Val87, Pro88, Ala90, Val91 and Met94 from α4, and of Phe101 and Glu103 from β5 (Figure 5). Additional contacts are provided by the mainchain atoms of Val99. The only polar interactions arise from the salt bridges between Lys95 from α4 in one protomer and Asp100 from β5 in the second protomer. The protein–protein contacts in the dimer are mainly hydrophobic, and the total change in solvent-accessible surface area amounts to 880 Å^2. Alanine-scanning mutagenesis of the receiver domain identified Val91 and Lys95 as being essential for phosphorylation-induced dimerization [24], which confirms that the interface containing helix α4 is the functional dimerization interface. Despite the unexpectedly small dimer interface area, we found no evidence, from isoelectric focusing (IEF) gels and over a few weeks, of dissociation of the phosphorylated dimer, which was also characterized by SAXS (beam line D24 at LURE, Orsay). The radius of gyration of a monodispersed solution of the dimer (R_g = 20.4 Å) was identical to that calculated from the X-ray structure, and significantly different from the one measured by the same method for the unphosphorylated FixJN monomer (R_g = 16.7 Å).

In the crystal structure of the phospho-FixJN dimer, the C termini of both receiver domains, at the ends of helices α5, point in the opposite direction relative to the surface containing the phosphorylation sites. This suggests that the two DNA-binding domains lie on the same side of the dimeric assembly in the full-length response regulator, allowing their simultaneous binding to promoter DNA [19]. Accordingly, the non-dimerizable mutated proteins FixJ V91A and K95A could be phosphorylated by acetyl-phosphate, but their affinities for the *fixK* promoter were decreased about tenfold as monitored by gel-shift assays [24]. Therefore both subunits of the phosphorylated dimer must interact in order to obtain a high DNA-binding affinity.

The residues at the dimer interface are poorly conserved among response regulators, except for Phe101 which is an aromatic residue in most proteins of this superfamily [12]. The equivalent residue in CheY, Tyr106, is involved in signal transduction [35], and it was proposed from behavioral and structural studies on CheY mutant proteins that the switching position of the Tyr106 sidechain would be modulated by the phosphorylation state of the molecule [36]. This hypothesis is supported by the conformational transition of Phe101 in FixJN from the unphosphorylated to the phosphorylated states. Phe101 may have the same signaling function in FixJ because the movement of the sidechain is required for

Figure 5

Stereoview of the dimer interface. One protomer is represented by black backbone atoms and grey sidechains. The second protomer is represented by magenta backbone atoms and lilac sidechains. The hydrogen bonds between Lys95 and Asp100 are represented by green dotted lines.

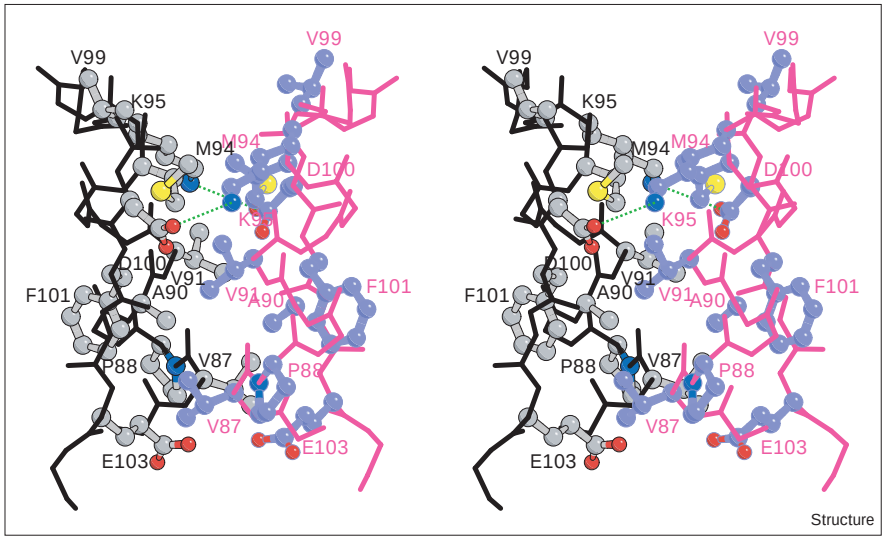

the formation of the dimer interface. This residue belongs to the C-terminal surface of the receiver domains, which is most affected by the phosphorylation-induced structural changes and is often referred to as the 'signaling surface' of response regulators. In several cases, this region has been shown to play an important role in triggering signal transduction to diverse targets. In CheY it mediates the binding to the flagellar motor switch proteins and to the kinase CheA [37]. In CheB this region modulates the functionality of the catalytic domain [9,38], and in NtrC it may control σ^{54} activating domains [34]. The X-ray structure of phosphorylated FixJN shows that other surface regions of the receiver domain, such as loops β1–α1 and β4–α4, sense phosphorylation and may therefore act in signal transduction. Interestingly, these two regions were shown to exhibit backbone dynamic motions in Spo0F [6,39] and to define the interaction surfaces with the cognate phosphorelay proteins [30,40].

Functional implications

The chemical stability of phosphorylated FixJ may be related to the specific protection of the acylphosphate group and to the extent of conformational changes of the protein, previously suggested as a means of stabilizing the phosphoaspartyl group within receiver domains [13]. The displacement of the His84 sidechain by 9 Å from its position in the unphosphorylated protein (Figure 4c) renders the phosphorous atom in phospho-FixJN inaccessible to a nucleophilic water molecule. These steric and electrostatic screening effects probably provide a significant contribution to the stability of the acylphosphate. In the other proteins of the response regulator superfamily, residues adjacent to the active site may have the same function. The lysine residue at position 56 in Spo0F was proposed to have a screening effect on the phosphoryl group, as its mutation to asparagine increased the autophosphatase activity of the protein [14]. In CheB the residue at the equivalent position is a glutamic acid. Its substitution by lysine reduces the rate of autodephosphorylation considerably [38].

Different molecular events may be required for response regulators to adopt their functionally activated states. Typical situations are illustrated by the two-domain response regulators NarL and CheB, which are negatively regulated by their receiver domains. The methylesterase CheB modulates the signaling activity of the bacterial chemotaxis receptors. The X-ray structure of the unphosphorylated full-length protein showed that the α4–β5–α5 surface of the receiver domain is tightly packed against the C-terminal domain, preventing access to its catalytic site [9]. The phosphorylation-induced conformational changes of this region illustrated in FixJ explain the disruption of this interface and the relieved inhibition of the catalytic domain [41]. In NarL the DNA-binding domain provides critical contacts to the receiver domain at the C-terminal parts of helices α3 and α4 [7]. Although this protein–protein interface is quite different from that found in CheB, it involves regions that relay the signal of phosphorylation (Figure 4a) and may favor the displacement of the output domain in phosphorylated NarL. In the case of FixJ, available data suggest a direct inhibitory interaction between the receiver domain and the transcription-activation domain [22,23]. It is straightforward to envision how the drastic conformational change demonstrated here may disrupt this interaction, thereby releasing DNA-binding activity of the FixJ C-terminal domain and resulting in transcriptional activation.

A sequence homology search, performed with the PSI-BLAST program [42] using the 82–101 sequence of FixJ as query, detected several response regulators. The sequence alignment of a selected set of proteins that display high conservation of residues at key positions in FixJN is given in Figure 6. One of these proteins is NtrC, the transcriptional activator of nitrogen assimilatory genes

Figure 6

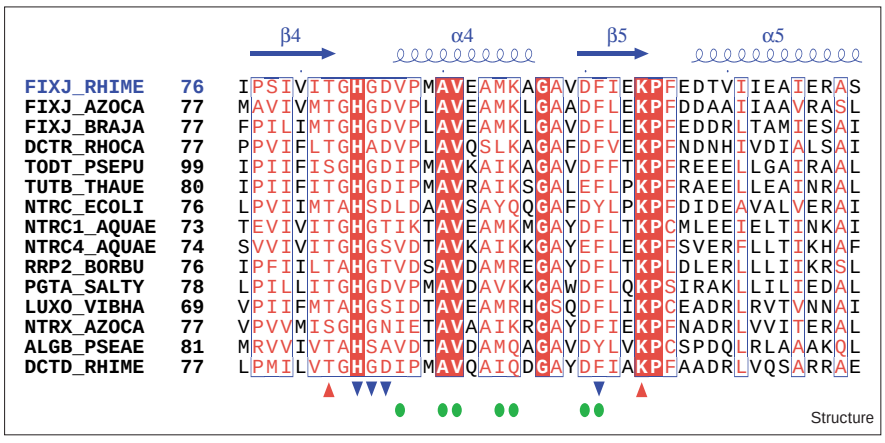

Alignment of sequences showing the highest conservation of key residues involved in the dimer interface. Sequences are ordered according to the subfamily of response regulators to which they belong: FixJ family from FIXJ_RHIME to TUTB_THAUE; NtrC family from NTRC_ECOLI to DCTD_RHIME. Symbols and color codes are the same as in Figure 1b.

[43]. Two mutations in NtrC, D86N and A89T outside the active site and the signaling surface of the receiver domain, were shown to additively increase the transcriptional activity of the unphosphorylated response regulator [34]. Asp86 and Arg56 are conserved in NtrC and FixJ. In FixJN the salt bridge and the hydrogen-bonding interactions between the sidechain of these two residues stabilize the conformation of the loop 83–86 (β4–α4) in the unphosphorylated form (Figure 3a). Upon phosphorylation, Asp86 shifts by 4.9 Å and moves close to residue 89. The alanine to threonine substitution at position 89 may stabilize the conformation of the β4–α4 loop observed in the phosphorylated structure via hydrogen-bonding interactions with the aspartic acid as well as with an asparagine at position 86. The two mutations may therefore additively favor a phosphorylated-like conformation of the receiver domain by switching the conformation of loop 83–86. The fact that the X-ray structure of phosphorylated FixJN and the NMR data on these activated NtrC mutant proteins show structural changes in identical regions of the receiver domains [34] suggests a link between the structural changes of the β4–α4 loop to those occurring at the signaling surface of the receiver domain.

The propagation of the conformational changes from the site of phosphorylation to adjacent regions in FixJN involves conserved residues and should therefore be similar in other receiver modules, possibly underlying the activation of response regulators. Sequence variations in a few areas may determine the stability of each conformation, the extent of the conformational change and therefore the signaling properties of various response regulators.

Biological implications

FixL/FixJ is the oxygen-sensitive two-component system involved in the regulation of symbiotic nitrogen fixation in *Sinorhizobium meliloti*. Under microaerobic conditions, phosphorylation of the response regulator FixJ by the kinase FixL induces dimerization of the protein and activates transcription of the *nifA* and *fixK* genes. FixJ displays a typical modular arrangement, with a phosphorylatable N-terminal receiver domain and a C-terminal DNA-binding domain. The receiver domains are conserved modules in all members of the response regulator superfamily, and their phosphorylation state controls the function of the output domains which display DNA-binding or enzymatic properties. Some response regulators are only produced as independent receiver modules. The three-dimensional structures of unphosphorylated response regulators revealed the conserved doubly wound five-stranded α/β fold of the receiver domains and the similarity of the active sites. They suggested a common mechanism of phosphorylation of the invariant aspartate residue, which alters the conformation of the protein and modulates the signaling properties. Here, we present the crystal structures of the phosphorylated and of the unphosphorylated receiver domain of FixJ solved at 2.3 Å and 2.4 Å resolution, respectively. These structures reveal the environment of the phosphoaspartate in the active site and the conformational changes induced by this chemical modification. The phosphorylation news propagates from the active site to the α4–β5 signaling surface of the receiver domain via a drastic conformational change of the β4–α4 loop region. This movement is driven by the polar interaction formed between the phosphoryl group and Thr82, an essential and always hydroxylated residue (serine or threonine) in this protein superfamily. This post-phosphorylation event allows the reorientation of Phe101, another highly conserved residue, and the molecular definition of the protein surface that mediates the dimerization of the response regulator. A single mutation in this interface decreases the affinity of the phosphorylated protein for the *fixK* promoter tenfold.

The observed conformational changes leading to activation of the response regulator by phosphorylation can be related to the genetic, biochemical and structural studies performed on other systems. We propose that they underlie the activation of response regulators in general.

Materials and methods

Protein expression and purification

The FixJN protein (residues 1–126 of FixJ with the T2Q and A125L mutations) was cloned in a pT7-7 plasmid and expressed in the *Escherichia coli* strain BL21(DE3)(pLysS). The bacterial pellet was lysed by sonication. The soluble fraction recovered by high-speed centrifugation was fractionated with ammonium sulfate before loading on a 16/100 Sephacryl S-100 gel-filtration column (Pharmacia). The FixJN protein, identified by sodium dodecyl sulfate polyacrylamide gel electrophoresis (SDS–PAGE) analysis, was then loaded onto a Q-sepharose column (Pharmacia) and eluted with a 0.1–0.5 M NaCl gradient. The fractions containing pure FixJN monomer were pooled, dialyzed and used for crystallization or for the preparation of the phosphorylated dimeric form. In the latter case, pure FixJN monomer was dialyzed against 20 mM Tris-HCl (pH 8.0), 100 mM NaCl, 0.1 mM dithiothreitol (DTT) and concentrated to 8–16 mg ml^{-1} using Centricon 10 (Amicon). Phosphorylated FixJN was prepared by incubating 0.4–0.8 mM pure FixJN monomer with 20 mM acetyl phosphate in 50 mM Tris-HCl (pH 7.2), 10 mM $MgCl_2$, 0.1 mM DTT for 2 h at 25°C. EDTA (10 mM) was then added to the mixture before loading onto a UnoQ6 column (Biorad). The protein was eluted with a 0–0.5 M NaCl gradient. Pure phosphorylated FixJN dimer was concentrated to 5 mg ml^{-1} using Centricon 10 in 20 mM Tris (pH 8.0), 250 mM NaCl, 1 mM EDTA, and 0.1 mM DTT.

Crystallization

Crystals were obtained at 4°C using the hanging-drop vapor-diffusion method. FixJN monomer in 20 mM Tris-HCl (pH 7.0), 0.1 mM EDTA, 1 mM DTT was concentrated to 12 mg ml^{-1} using Centricon 10. The protein solution (2 µl) was mixed with an equal volume of the reservoir solution, which contained 40% (w/v) polyethylene glycol (PEG) 1500 in 20 mM Tris-HCl (pH 7.0). After three months, the crystal dimensions were about $150 \times 50 \times 20$ μm^3. Crystals were directly cryocooled in liquid propane. The crystals belong to the space group P1, with unit-cell dimensions a = 31.7 Å, b = 42.2 Å, c = 44.6 Å, α = 93.2°, β = 104.5° and γ = 101.9°, and contain two molecules per asymmetric unit for a solvent content of 30%. Heavy-atom derivatives were obtained by soaking crystals in a 4 mM $Sm(NO_3)_3$ solution for 48 h, or a 8 mM K_2PtCl_4 solution for 15 h. For crystals of phosphorylated FixJN, the

protein solution (2 µl) was mixed with an equal volume of the reservoir solution, which contained 2.0 M ammonium sulfate, 100 mM Hepes (pH 7.5), 1 mM EDTA. After three days, 10% 2-methyl-2,4 pentanediol (MPD) (v/v) was added to the reservoir, and 1 µl of 0.056% (w/v) Triton X-100, 1.6 M ammonium sulfate, 10% MPD, 80 mM Hepes (pH 7.5), 0.8 mM EDTA was added to the crystallization drop. Thin plate-like crystals grew within one month. Cryoprotection was achieved by transferring the crystals, for five minutes, in a drop (1 µl) containing 25% sucrose, 15% glycerol, 1.5 M ammonium sulfate, 88 mM Hepes (pH 7.5), 1 mM EDTA. The crystals were flash cooled in a nitrogen stream, and stored in propane at liquid-nitrogen temperature. The crystals belong to the space group C2 with unit-cell dimensions a = 132.1 Å, b = 91.3 Å, c = 59.9 Å, $\beta = 112.4°$, and contain three molecules per asymmetric unit for a solvent content of 68%. Data sets were collected at –178°C on the synchrotron beam lines ID14-EH3 and ID14-EH4 at ESRF (Grenoble). Data were processed and scaled with MOSFLM [44] and SCALA [45] or with DENZO/SCALEPACK [46].

Structure determinations, model building, and refinement

The structure of the unphosphorylated FixJN was solved by the MIRAS method. The anomalous contribution of the samarium derivative was determinant for phasing, which was performed with the program SHARP [47]. The resulting figure of merit was equal to 0.52 for data to 2.4 Å resolution (Table 1). Subsequent cycles of density modification with the program DM [45] using noncrystallographic twofold averaging led to a map of good quality (final real space coefficient correlation [Cc] equal to 94%) from which the characteristic trace of the receiver domain was clearly visible. Model building and corrections were carried out using TURBO-FRODO [48]. The structures were refined with the program CNS [49] (Table 1).

The structure of the phosphorylated FixJN dimer (Table 2) was solved by molecular replacement using AMoRe [50] and the structure of the unphosphorylated FixJN domain as a search model. It yielded solutions for three molecules in the asymmetric unit with R factor and Cc of 0.435 and 49.7% (15–3.5 Å), respectively. The three molecules in the asymmetric unit are related by two noncrystallographic twofold axes in agreement with a self-rotation function. The phases derived from the molecular replacement model were improved by solvent flattening and noncrystallographic-symmetry averaging using DM [45]. Structure refinement was performed using CNS [49]. Anisotropic B factor and bulk-solvent corrections as well as the cross-validation method [51] were applied throughout the refinement. Initially, only 2.8 Å resolution data were included for refinement with tight noncrystallographic-symmetry restraints (300 kcal mol^{-1} $Å^2$), and manual rebuilding was carried out in averaged electron-density maps. These restraints were abandoned when the resolution limit was extended to 2.3 Å. Hereafter, the models were inspected in SIGMAA [52] weighted maps. The electron densities of the phosphoryl group on each protomer were the three highest positive peaks (14.0σ) in the F_o–F_c SIGMAA weighted map. The phosphoryl groups were introduced at that stage. Several rounds of solvent positioning, with density higher than 4.0σ, and model corrections were finally carried out. The final model comprises 122 to 123 out of 126 residues in the recombinant protein, three phosphoryl groups attached to Asp54, four sulfate ions, and 144 water molecules. The crystallographic R factor is 0.217 (R_{free} = 0.244) for all measurements between 24.5 and 2.3 Å (Table 2). All residues are in the allowed regions of a Ramachandran plot and 91.9% of them have the most favored backbone ϕ,ψ angles, as defined by PROCHECK [53]. The average B factors are 42.3 $Å^2$ for protein atoms (39.9 $Å^2$ for mainchain atoms, 44.2 $Å^2$ for sidechain atoms, 40.0 $Å^2$ for phosphoryl atoms) and 48.8 $Å^2$ for solvent atoms.

Figures 1a, 2, 3, 4a, 4c, 5 were produced with BOBSCRIPT [54]. Figures 1a and 2 were rendered in Raster3D [55].

Accession numbers

The coordinates and structure factors for the phosphorylated FixJN dimer have been deposited in the Protein Data Bank with accession code 1D5W and are on hold until 12 October 2000.

Acknowledgements

We thank the scientific staff of ESRF (Grenoble, France) and LURE (Orsay, France) for excellent data collection facilities, V Guillet for contributions in data collection and E Courcelle for computing facilities. This work was supported by grants from the European Union (BIO4 CT 97-2143) and the Ministère de l'Education Nationale, de la Recherche et de la Technologie (Programme de Recherche Fondamentale en Microbiologie et Maladies Infectieuses et Parasitaires).

References

1. Parkinson, J.S. & Kofoid, E.C. (1992). Communication modules in bacterial signaling proteins. *Annu. Rev. Genet.* **26**, 71-112.
2. Asayama, M., Yamamoto, A. & Kobayashi, Y. (1995). Dimer form of phosphorylated Spo0A, a transcriptional regulator, stimulates the *spo0F* transcription at the initiation of sporulation in *Bacillus subtilis*. *J. Mol. Biol.* **250**, 11-23.
3. Stock, A.M., *et al.,* & Petsko, G.A. (1993). Structure of the $Mg^{(2+)}$-bound form of CheY and mechanism of phosphoryl transfer in bacterial chemotaxis. *Biochemistry* **32**, 13375-13380.
4. Bellsolell, L., Prieto, J., Serrano, L. & Coll, M. (1994). Magnesium binding to the bacterial chemotaxis protein CheY results in large conformational changes involving its functional surface. *J. Mol. Biol.* **238**, 489-495.
5. Volkman, B.F., Nohaile, M.J., Amy, N.K., Kustu, S. & Wemmer, D.E. (1995). Three-dimensional solution structure of the N-terminal receiver domain of NTRC. *Biochemistry* **34**, 1413-1424.
6. Feher, V.A., Zapf, J.W., Hoch, J.A., Dahlquist, F.W., Whiteley, J.M. & Cavanagh, J. (1995). 1H, 15N, and 13C backbone chemical shift assignments, secondary structure, and magnesium-binding characteristics of the *Bacillus subtilis* response regulator, Spo0F, determined by heteronuclear high-resolution NMR. *Protein Sci.* **4**, 1801-1814.
7. Baikalov, I., Schroder, I., Kaczor-Grzeskowiak, M., Grzeskowiak, K., Gunsalus, R.P. & Dickerson, R.E. (1996). Structure of the *Escherichia coli* response regulator NarL. *Biochemistry* **35**, 11053-11061.
8. Madhusudan, M., Zapf, J., Hoch, J.A., Whiteley, J.M., Xuong, N.H. & Varughese, K.I. (1997). A response regulatory protein with the site of phosphorylation blocked by an arginine interaction: crystal structure of Spo0F from *Bacillus subtilis*. *Biochemistry* **36**, 12739-12745.
9. Djordjevic, S., Goudreau, P.N., Xu, Q., Stock, A.M. & West, A.H. (1998). Structural basis for methylesterase CheB regulation by a phosphorylation-activated domain. *Proc. Natl Acad. Sci. USA* **95**, 1381-1386.
10. Solà, M., Gomis, F., Serrano, L., Gonzalez, A. & Coll, M. (1999). Three-dimensional crystal structure of the transcription factor PhoB receiver domain. *J. Mol. Biol.* **285**, 675-687.
11. Lukat, G.S., Stock, A.M. & Stock, J.B. (1990). Divalent metal ion binding to the CheY protein and its significance to phosphotransfer in bacterial chemotaxis. *Biochemistry* **29**, 5436-5442.
12. Volz, K. (1993). Structural conservation in the CheY superfamily. *Biochemistry* **32**, 11741-11753.
13. Stock, J.B., Surette, M.G., Levit, M. & Park, P. (1995). Structure-Function Relationships and Mechanisms of Catalysis. In *Two-Component Signal Transduction* (Hoch, J.A. & Silhavy, T., eds), pp 25-51, ASM Press, Washington D.C.
14. Zapf, J., Madhusudan, M., Grimshaw, C.E., Hoch, J.A., Varughese, K.I. & Whiteley, J.M. (1998). Source of response regulator autophosphatase activity: the critical role of a residue adjacent to the Spo0F autophosphorylation active site. *Biochemistry* **37**, 7725-7732.
15. Goudreau, P.N. & Stock, A.M. (1998). Signal transduction in bacteria: molecular mechanisms of stimulus-response coupling. *Curr. Opin. Microbiol.* **1**, 160-169.
16. David, M., *et al.,* & Kahn, D. (1988). Cascade regulation of gene expression in *Rhizobium meliloti*. *Cell* **54**, 671-683.
17. Agron, P.G. & Helinski, D.R. (1995). Symbiotic expression of *Rhizobium meliloti* nitrogen fixation genes is regulated by oxygen. In *Two-Component Signal Transduction* (Hoch, J.A. & Silhavy, T., eds), pp 275-287, ASM Press, Washington D.C.
18. Waelkens, F.A., Foglia, A., Morel, J.-B., Fourment, J., Batut, J. & Boistard, P. (1992). Molecular genetic analysis of the *Rhizobium meliloti fixK* promoter: identification of sequences involved in positive and negative regulation. *Mol. Microbiol.* **6**, 1447-1456.
19. Galinier, A., Garnerone, A.-M., Reyrat, J.-M., Kahn, D., Batut, J. & Boistard, P. (1994). Phosphorylation of the *Rhizobium meliloti* FixJ protein induces its binding to a compound regulatory region at the *fixK* promoter. *J. Biol. Chem.* **269**, 23784-23789.

20. Agron, P.G., Ditta, G.S. & Helinski, D.R. (1993). Oxygen regulation of *nifA* transcription *in vitro*. *Proc. Natl Acad. Sci. USA* 90, 3506-3510.
21. Reyrat, J.M., David, M., Blonski, C., Boistard, P. & Batut, J. (1993). Oxygen-regulated *in vitro* transcription of *Rhizobium meliloti nifA* and *fixK* genes. *J. Bacteriol.* 175, 6867-6872.
22. Kahn, D. & Ditta, G. (1991). Modular structure of FixJ: homology of the transcriptional activator domain with the -35 binding domain of sigma factors. *Mol. Microbiol.* 5, 987-997.
23. Da Re, S., Bertagnoli, S., Fourment, J., Reyrat, J.-M. & Kahn, D. (1994). Intramolecular signal transduction within the FixJ transcriptional activator: in vitro evidence for the inhibitory effect of the phosphorylatable regulatory domain. *Nucleic Acids Res.* 22, 1555-1561.
24. Da Re, S., Schumacher, J., Rousseau, P., Fourment, J., Ebel, C. & Kahn, D. (1999). Phosphorylation-induced dimerisation of the FixJ receiver domain. *Mol. Microbiol.* 34, 504-511.
25. Weinstein, M., Lois, A.F., Ditta, G.S. & Helinski, D.R. (1993). Mutants of the two-component regulatory protein FixJ of *Rhizobium meliloti* that have increased activity at the *nifA* promoter. *Gene* 134, 145-152.
26. Welch, M., Chinardet, N., Mourey, L., Birck, C. & Samama, J.P. (1998). Structure of the CheY-binding domain of histidine kinase CheA in complex with CheY. *Nat. Struct. Biol.* 5, 25-29.
27. Lukat, G.S., Lee, B.H., Mottonen, J.M., Stock, A.M. & Stock, J.B. (1991). Roles of the highly conserved aspartate and lysine residues in the response regulator of bacterial chemotaxis. *J. Biol. Chem.* 266, 8348-8354.
28. Brissette, R.E., Tsung, K.L. & Inouye, M. (1991). Suppression of a mutation in OmpR at the putative phosphorylation center by a mutant EnvZ protein in *Escherichia coli*. *J. Bacteriol.* 173, 601-608.
29. Weinstein, M., Lois, A.F., Monson, E.K., Ditta, G.S. & Helinski, D.R. (1992). Isolation of phosphorylation-deficient mutants of the *Rhizobium meliloti* two-component regulatory protein, FixJ. *Mol. Microbiol.* 6, 2041-2049.
30. Tzeng, Y.L. & Hoch, J.A. (1997). Molecular recognition in signal transduction : the interaction surfaces of the Spo0F response regulator with its cognate phosphorelay proteins revealed by alanine scanning mutagenesis. *J. Mol. Biol.* 272, 200-212.
31. Appleby, J.L. & Bourret, R.B. (1998). Proposed signal transduction role for conserved CheY residue Thr87, a member of the response regulator active-site quintet. *J. Bacteriol.* 180, 3563-3569.
32. Drake, S.K., Bourret, R.B., Luck, L.A., Simon, M.I. & Falke, J.J. (1993). Activation of the phosphosignaling protein CheY. I. Analysis of the phosphorylated conformation by 19F NMR and protein engineering. *J. Biol. Chem.* 268, 13081-13088.
33. Lowry, D.F., *et al.* & Matsumura, P. (1994). Signal transduction in chemotaxis. A propagating conformation change upon phosphorylation of CheY. *J. Biol. Chem.* 269, 26358-26362.
34. Nohaile, M., Kern, D., Wemmer, D., Stedman, K. & Kustu, S. (1997). Structural and functional analyses of activating amino acid substitutions in the receiver domain of NtrC: evidence for an activating surface. *J. Mol. Biol.* 273, 299-316.
35. Zhu, X., Amsler, C.D., Volz, K. & Matsumura, P. (1996). Tyrosine 106 of CheY plays an important role in chemotaxis signal transduction in *Escherichia coli*. *J. Bacteriol.* 178, 4208-4215.
36. Zhu, X., Rebello, J., Matsumura, P. & Volz, K. (1997). Crystal structures of CheY mutants Y106W and T87I/Y106W. CheY activation correlates with movement of residue 106. *J. Biol. Chem.* 272, 5000-5006.
37. Djordjevic, S. & Stock, A.M. (1998). Structural analysis of bacterial chemotaxis proteins: components of a dynamic signaling system. *J. Struct. Biol.* 124, 189-200.
38. Stewart, R.C. (1993). Activating and inhibitory mutations in the regulatory domain of CheB, the methylesterase in bacterial chemotaxis. *J. Biol. Chem.* 268, 1921-1930.
39. Feher, V.A., Tzeng, Y.L., Hoch, J.A. & Cavanagh, J. (1998). Identification of communication networks in Spo0F: a model for phosphorylation-induced conformational change and implications for activation of multiple domain bacterial response regulators. *FEBS Lett.* 425, 1-6.
40. Varughese, K.I., Madhusudan, M., Zhou, X.Z., Whiteley, J.M. & Hoch, J.A. (1998). Formation of a novel four-helix bundle and molecular recognition sites by dimerization of a response regulator phosphotransferase. *Mol. Cell* 2, 485-493.
41. Lupas, A. & Stock, J. (1989). Phosphorylation of an N-terminal regulatory domain activates the CheB methylesterase in bacterial chemotaxis. *J. Biol. Chem.* 264, 17337-17342.
42. Altschul, S.F., *et al.,* & Lipman, D.J. (1997). Gapped BLAST and PSI-BLAST: a new generation of protein database search programs. *Nucleic Acids Res.* 25, 3389-3402.
43. Magasanik, B. (1988). Reversible phosphorylation of an enhancer binding protein regulates the transcription of bacterial nitrogen utilization genes. *Trends Biochem. Sci.* 13, 475-479.
44. Leslie, A.G.W. (1987). Computational aspects of protein crystal data analysis. In *Proceedings of the Daresbury Study Weekend* (Helliwell, J.R., Machin, P.A. & Papiz, M.Z., eds), pp 39-50, SERC, Daresbury Laboratory, Warrington, UK.
45. Collaborative Computational Project, Number 4. (1994). The CCP4 suite: programs for protein crystallography. *Acta Crystallogr. D* 50, 760-763.
46. Otwinowski, Z.O. & Minor, W. (1997). Processing of X-ray diffraction data collected in oscillation mode. *Methods Enzymol.* 276, 307-326.
47. de La Fortelle, E. & Bricogne, G. (1997). Maximum-likelihood heavy-atom parameter refinement for multiple isomorphous replacement and multiwavelength anomalous diffraction methods. *Methods Enzymol.* 276, 472-494.
48. Roussel, A. & Cambillau, C. (1989). The TURBO-FRODO Graphics Package. In *Silicon Graphics Geometry Partners Directory* (Silicon Graphics, ed.), vol. 81, pp 71-78, Silicon Graphics, Mountain View, CA.
49. Brünger, A.T., *et al.,* & Warren, G.L. (1998). Crystallography & NMR system: A new software suite for macromolecular structure determination. *Acta Crystallogr. D* 54, 905-921.
50. Navaza, J. (1994). AMoRe: an automated package for molecular replacement. *Acta Crystallogr. A* 50, 157-163.
51. Brünger, A.T. (1992). Free R value: a novel statistical quantity for assessing the accuracy of crystal structures. *Nature* 355, 472-475.
52. Read, R.J. (1986). Improved Fourier coefficients for maps using phases from partial structures with errors. *Acta Crystallogr. A* 42, 140-149.
53. Laskowski, R.A., MacArthur, M.W., Moss, D.S. & Thornton, J.M. (1993). PROCHECK: a program to check the stereochemical quality of protein structures. *J. Appl. Crystallogr.* 26, 283-291.
54. Esnouf, R.M. (1997). An extensively modified version of MOLSCRIPT that includes greatly enhanced coloring capabilities. *J. Mol. Graph.* 15, 133-138.
55. Merritt, E.A. & Murphy, M.E.P. (1994). Raster3D version 2.0 – a program for photorealistic molecular graphics. *Acta Crystallogr. D* 50, 869-873.
56. Volz, K. & Matsumura, P. (1991). Crystal structure of *Escherichia coli* CheY refined at 1.7 Å resolution. *J. Biol. Chem.* 266, 15511-15519.
57. Gouet, P., Courcelle, E., Stuart, D. & Metoz, F. (1998). ESPript: multiple sequence alignments in PostScript. *Bioinformatics* 15, 305-308.
58. Laskowski, R.A. (1995). SURFNET: a program for visualizing molecular surfaces, cavities and intermolecular interactions. *J. Mol. Graph.* 13, 323-330.

Because *Structure with Folding & Design* operates a 'Continuous Publication System' for Research Papers, this paper has been published on the internet before being printed (accessed from http://biomednet.com/cbiology/str). For further information, see the explanation on the contents page.